Original Article

PMP

Progress in Medical Physics 32(4), December 2021
https://doi.org/10.14316/pmp.2021.32.4.92
eISSN 2508-4453

Estimation of Noise Level and Edge Preservation for Computed Tomography Images: Comparisons in Iterative Reconstruction

Sihwan Kim[1], Chulkyun Ahn[2], Woo Kyoung Jeong[3], Jong Hyo Kim[1,4,5,6,7], Minsoo Chun[7,8]

[1]Department of Applied Bioengineering, Graduate School of Convergence Science and Technology, Seoul National University, [2]Department of Transdisciplinary Studies, Program in Biomedical Radiation Sciences, Graduate School of Convergence Science and Technology, Seoul National University, [3]Department of Radiology, Samsung Medical Center, Sungkyunkwan University School of Medicine, [4]Department of Radiology, Seoul National University Hospital, Seoul National University College of Medicine, [5]ClariPi Research, Seoul, [6]Center for Medical-IT Convergence Technology Research, Advanced Institutes of Convergence Technology, Suwon, [7]Institute of Radiation Medicine, Seoul National University Medical Research Center, [8]Department of Radiation Oncology, Chung-Ang University Hospital, Seoul, Korea

Received 8 December 2021
Revised 15 December 2021
Accepted 20 December 2021

Corresponding author
Minsoo Chun
(ms1236@caumc.or.kr)
Tel: 82-2-6299-2673
Fax: 82-2-3280-2674

Purpose: This study automatically discriminates homogeneous and structure edge regions on computed tomography (CT) images, and it evaluates the noise level and edge preservation ratio (EPR) according to the different types of iterative reconstruction (IR).

Methods: The dataset consisted of CT scans of 10 patients reconstructed with filtered back projection (FBP), statistical IR (iDose^4), and iterative model-based reconstruction (IMR). Using the 10th and 85th percentiles of the structure coherence feature, homogeneous and structure edge regions were localized. The noise level was estimated using the averages of the standard deviations for five regions of interests (ROIs), and the EPR was calculated as the ratio of standard deviations between homogeneous and structural edge regions on subtraction CT between the FBP and IR.

Results: The noise levels were 20.86±1.77 Hounsfield unit (HU), 13.50±1.14 HU, and 7.70±0.46 HU for FBP, iDose^4, and IMR, respectively, which indicates that iDose^4 and IMR could achieve noise reductions of approximately 35.17% and 62.97%, respectively. The EPR had values of 1.14±0.48 and 1.22±0.51 for iDose^4 and IMR, respectively.

Conclusions: The iDose^4 and IMR algorithms can effectively reduce noise levels while maintaining the anatomical structure. This study suggested automated evaluation measurements of noise levels and EPRs, which are important aspects in CT image quality with patients' cases of FBP, iDose^4, and IMR. We expect that the inclusion of other important image quality indices with a greater number of patients' cases will enable the establishment of integrated platforms for monitoring both CT image quality and radiation dose.

Keywords: Computed tomography, Image quality, Subtraction image, Noise level, Structure edge preservation

Introduction

Over the past several decades, computed tomography (CT) imaging techniques have been developed in various ways. One of the most important concerns in CT imaging is the balance between radiation dose and image quality [1].

The importance of reducing radiation doses while maintaining image quality has led to technical improvements, such as automatic exposure control, iterative reconstruction (IR), and dual-energy imaging techniques [2-5]. Furthermore, IR techniques are widely used in clinics, and they have replaced the conventional filtered back projection (FBP) method [6]. IR updates the image estimate through iterative numerical calculations until the errors between the calculated and measured data are minimized and converge [7]. Compared with the FBP method using an analytic approach, it is robust against quantum noise and artifacts. Recently, an image reconstruction technique based on deep learning has emerged, creating a new paradigm [8,9]. Deep learning reconstruction (DLR) is a data-driven approach that produces images with lower image noise than those reconstructed using the IR method [10,11]. In addition, it performs the task in a shorter time with respect to the image processing speed. Currently, many state-of-the-art reconstruction algorithms are based on deep learning, and they support radiological image-reading tasks.

Although IR and DLR can effectively reduce image noise, over-smoothing of small-scale structures, and alteration of image textures are inevitable. Although the amount of IR-aided noise reduction is visually clear, their quantification is necessary because human observers often fail to discern subtle differences [3]. Furthermore, intra- and interobserver variabilities affect image quality evaluation, specifically for those with large differences in experience. Although evaluations of noise reductions are an efficient way to demonstrate the improvements of image quality from IR, they also depend on raters and circumstances, as it is necessary to manually place regions of interest (ROI) in homogeneous areas. Subtraction CT (SCT) between reference (usually FBP) and IR images may provide insights for the quantification of residual structures [12,13]. When IR operates well, which reduces noise levels while preserving the anatomical structures, subtraction domains present noise-only images [8,9]. Contrarily, there are substantial residual components in the subtraction domain if the IR poorly works. We reported that the use of low-level thresholds of the structure coherence features (SCFs) could effectively localize homogeneous areas [14]. Moreover, the use of a higher SCF enables the identification of structural transition regions. This study demonstrates the quantification of SCT-based image quality using commercially available statistical and model-based IR.

Materials and Methods

1. Dataset

The abdominopelvic CT images of 10 patients with post contrast phases were retrospectively selected after obtaining Institutional Review Board of the Seoul National University Hospital approval (IRB No. 1905–077–1033). Informed consent was not required in this study because only image data were used and they presented minimal risk of harm to subjects. The CT datasets were acquired using a multi-detector CT scanner (iCT, Philips Healthcare, Cleveland, OH, USA), and they were reconstructed with conventional FBP, statistical IR (iDose^4, Philips Healthcare), and iterative model-based reconstruction (IMR, Philips Healthcare). The scanning parameters were tube voltage of 100 kVp and slice thickness of 3 mm; automatic exposure control option was applied, showing a tube current time product (mAs) of 131.64±1.86.

2. Reference tissue segmentation

The hepatic parenchyma tissue was used as the reference tissue for the quantification of image quality [15]. Gaussian filtering with a sigma value of 2.5 was performed to mitigate the noise effect on the reference tissue segmentation. Using the geometrical and intensity information of the liver parenchyma, the initial seed was located at the upper-right end of the image. If the initial seed was lower than 0 Hounsfield unit (HU), two pixel steps moved it until the corresponding pixel values were greater than 0 HU. With this seed point, the reference tissue was acquired via three-dimensional region growing, hole-filling, and morphological operation (Fig. 1b).

3. Structure coherence feature and extraction of homogeneous and edge transition region

Previously, we proposed a SCF, which consists of an edgi-

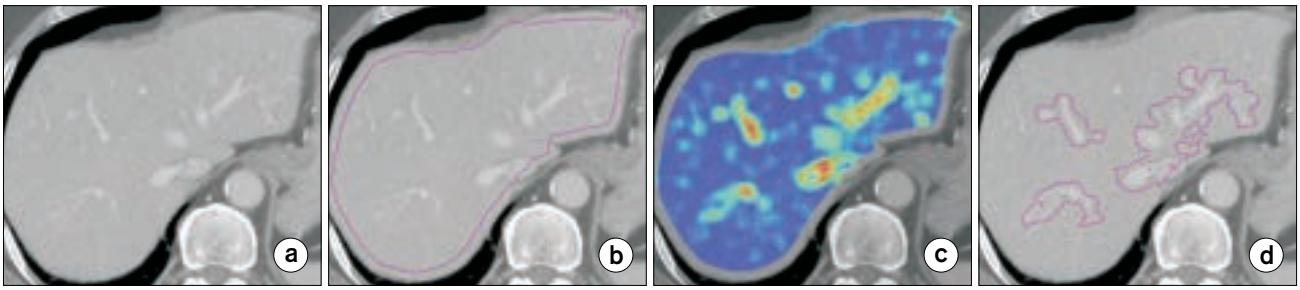

Fig. 1. Procedures to extract structural transition region in enhanced hepatic region. (a) Original image, (b) candidate evaluation mask, (c) SCF map, and (d) edge regions extracted using SCF threshold greater than the 85th percentile. SCF, structure coherence feature.

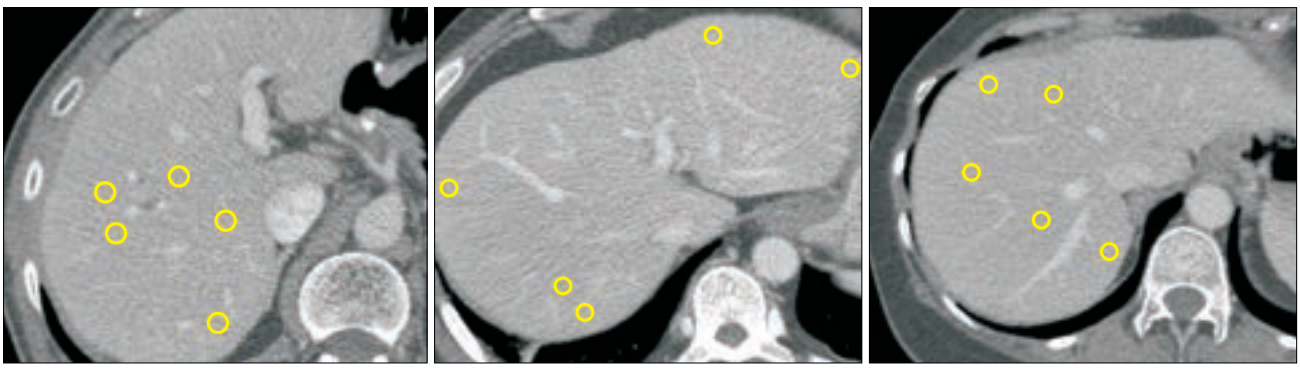

Fig. 2. Sample results of ROI placement on homogeneous area on the liver parenchyma. ROI, regions of interest.

ness feature to represent the likelihood of a pixel being located on an anatomical structure and the randomness of the pixel orientation to represent the absence of an anatomical structure [14]. The SCF was defined as follows:

$$f_S = \frac{\sum_{(i,j)\in ROI} I_E(i,j)}{H_G + H_T}, \quad (1)$$

where I_E, H_G, and H_T denote the edginess of each pixel as well as the directional entropy for the gradient vector and structure tensor, respectively [14]. The circular ROIs with an area of less than 1 cm^2 were used [16]. The structural edges between two different tissues were extracted by applying a high SCF threshold. We empirically found that the 85th percentile of the SCF was appropriate for localizing the structure transition region, and we named it R_S. Regions with SCF less than the 10th percentile belonged to the homogeneous area, and they were named as R_H.

4. Noise level estimation and preservation of an organ structure

For R_H, the standard deviations of five randomly selected ROIs were averaged to calculate the representative noise levels. The placement of the five homogeneous ROIs was visually evaluated. In the subtraction domain between the reference (FBP) and IR images, the standard deviation values of the ROIs with pure noise were lower compared with those containing structural edges. Therefore, we defined the edge preservation ratio (EPR) as follows:

$$EPR = \left.\frac{\sigma_{R_S}}{\sigma_{R_H}}\right|_{\Delta I}, \quad (2)$$

where σ denotes the standard deviation, the subscript denotes the regions being evaluated, and ΔI indicates the subtraction domain. Hence, the EPR value will be approximately one when the advanced reconstruction algorithm reduces the noise without degrading the structural components. Contrarily, the EPR decreases if substantial residual

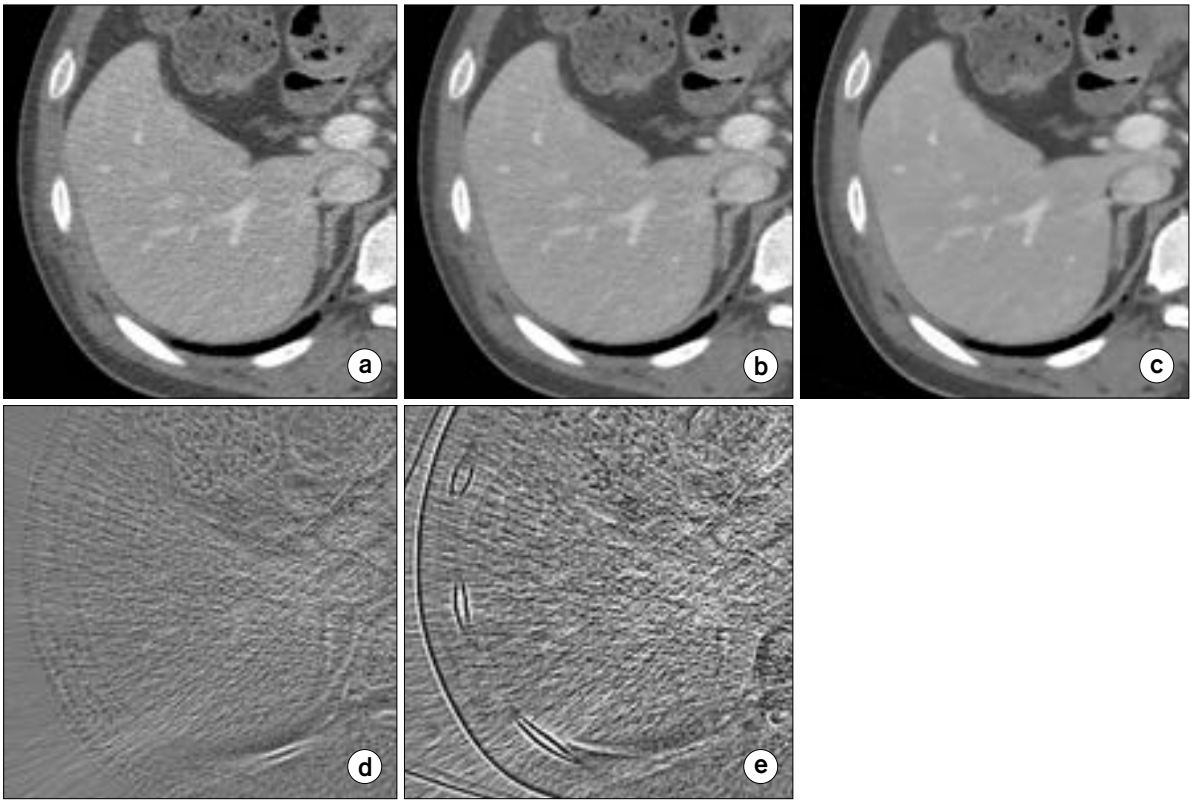

Fig. 3. Sample images reconstructed with (a) FBP, (b) iDose[4], and (c) IMR. SCT between (d) FBP and iDose[4] as well as (e) FBP and IMR. FBP, filtered back projection; IMR, iterative model-based reconstruction; SCT, subtraction computed tography.

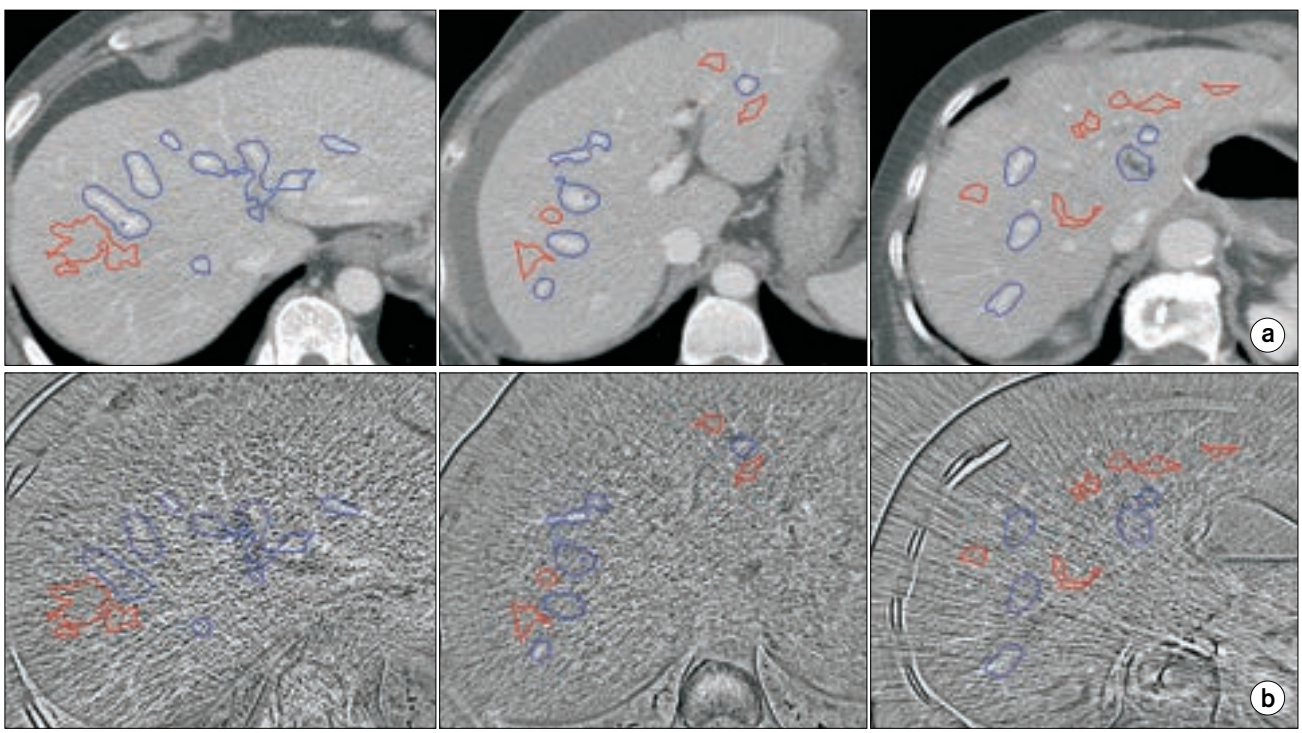

Fig. 4. Sample localization results of homogeneous (red) and structure transition (blue) regions displayed on (a) FBP image and (b) SCT domain. FBP, filtered back projection; SCT, subtraction computed tography.

structures exist in the subtraction image domain.

Results

1. Noise level

All ROIs were successfully located in homogeneous regions, and the sample ROI placements are presented in Fig. 2. The noise levels were 20.86±1.77 HU, 13.50±1.14 HU, and 7.70±0.46 HU for FBP, iDose^4, and IMR, respectively. The noise levels were reduced by approximately 35.17% and 62.97% using iDose^4 and IMR, respectively.

2. Edge preservation ratio

In the SCT domain for both iDose^4 and IMR, the residual structures and streak appearances are shown, and their amounts are difficult to quantify with the human eye (Fig. 3). Automated extraction of homogeneous and structure transition regions are presented in Fig. 4. The EPR showed values of 1.14±0.48 and 1.22±0.51 for iDose^4 and IMR, respectively.

Discussion

In this study, we quantified the amount of structural preservation induced by IR using SCT between FBP and IRs, which consist of both statistical and model-based approaches. The EPR values for iDose^4 and IMR demonstrated reliable quantification with visual assessments on SCT.

SCT is widely used in clinics for various applications. Subtraction across adjacent images is often applied to predict the noise levels [17]. Although the two subsequent CT images are correlated, the average discrepancy in noise measurements between the single-image dataset and subtraction domains showed errors of less than 1% on average [17]. In phantom or cadaver images, it is more suitable to scan objects repeatedly. Multiple scans and their subtractions have been demonstrated to provide reliable noise estimates [17,18]. In the SCT application across different scans, Onoue et al. [19] reported that temporal SCT with nonrigid image registration improves the detection of metastases by six board-certified radiologists. Metal artifact reduction (MAR) algorithms extract the sinograms of high-density metal from those of the original and priors; then, they restore them with post processing via an edge-preserving filter and a recovery of the adjacent anatomical structures [13,20]. Although there are no standard evaluation techniques, visual scoring, spicularity at the lines crossing the metal region, mean or standard deviation of HU near metals, the percent integrity uniformity, or coefficients of fast Fourier transform on the ROIs in close vicinity of the materials are widely employed [21,22]. SCTs between the original and MAR-corrected images can provide an indication of visible object edges and other structural information aside from the artifacts [23]. Based on the type of SCT, this evaluation strategy is applicable to either phantom only or both phantom and clinical images because multiple scans on patient's increases radiation-induced complications. Evidently, SCT can be effectively used for image quality evaluation.

This study has several limitations. First, the number of patients was relatively small, and the images obtained using a single CT scanner were used. Currently, there are many reconstruction techniques, including IR and DLR. According to the types and manufacturers of IRs and DLRs, the amount of noise reduction and texture appearances are completely different. We plan to evaluate multiple types of IRs and DLRs with a greater number of patients. Second, other types of image quality metrics were not evaluated. Many parameters affect the diagnostic performance. Specifically, noise is a primary factor in terms of both the noise level and the noise power spectrum [24]. The nonlinear properties of IR and nonexplainable problems of DLR should be evaluated using appropriate evaluation approaches [25-28]. The limitations on the application of noise power spectrum measurements with patient images can be replaced using an estimation of the noise grain size [29]. The use of other image quality metrics along with radiation dose assessment could provide a more reliable and integrated image quality evaluation.

Currently, the concept of diagnostic reference level in CT is changing to that of noise and dose reference levels. Therefore, emphasis on not only the radiation dose but also the image quality will become more prevalent. We expect our study to be an initial attempt toward the integration of the assessment of CT image quality and radiation dose,

which would make it possible to lead a patient-friendly society.

Conclusions

This study employs SCT to localize homogeneous and structural edge regions and visually assess their placements. Furthermore, the noise level and residual structure according to iDose[4] and IMR were evaluated in a fully automated manner. This automated measurement technique can contribute to the development of a nationwide CT image quality management program.

Acknowledgements

This work was supported by the Korea Medical Device Development Fund grant funded by the Korea government (the Ministry of Science and ICT, the Ministry of Trade, Industry and Energy, the Ministry of Health & Welfare, Republic of Korea, the Ministry of Food and Drug Safety) (Project Number: 1711138600, 1711138601, KMDF_PR_20200901_0267).

Conflicts of Interest

The authors have nothing to disclose.

Availability of Data and Materials

All relevant data are within the paper and its Supporting Information files.

Author Contributions

Conceptualization: Jong Hyo Kim and Minsoo Chun. Data curation: Woo Kyoung Jeong. Formal analysis: Sihwan Kim, Chulkyun Ahn, and Minsoo Chun. Funding acquisition: Minsoo Chun. Investigation: Sihwan Kim and Chulkyun Ahn. Methodology: Minsoo Chun and Sihwan Kim. Project administration: Minsoo Chun. Resources: Chulkyun Ahn and Minsoo Chun. Software: Jong Hyo Kim, Sihwan Kim, and Minsoo Chun. Supervision: Jong Hyo Kim and Minsoo Chun. Validation: Woo Kyoung Jeong. Visualization: Sihwan Kim and Minsoo Chun. Writing–original draft: Minsoo Chun, Sihwan Kim, and Chulkyun Ahn. Writing–review & editing: Jong Hyo Kim and Minsoo Chun.

References

1. ICRP, Khong PL, Ringertz H, Donoghue V, Frush D, Rehani M, et al. ICRP publication 121: radiological protection in paediatric diagnostic and interventional radiology. Ann ICRP. 2013;42:1-63.
2. Söderberg M, Gunnarsson M. Automatic exposure control in computed tomography--an evaluation of systems from different manufacturers. Acta Radiol. 2010;51:625-634.
3. Singh S, Kalra MK, Thrall JH, Mahesh M. Automatic exposure control in CT: applications and limitations. J Am Coll Radiol. 2011;8:446-449.
4. Ha S, Jung S, Chang HJ, Park EA, Shim H. Effects of iterative reconstruction algorithm, automatic exposure control on image quality, and radiation dose: phantom experiments with coronary CT angiography protocols. Prog Med Phys. 2015;26:28-35.
5. Ju EB, Ahn SH, Choi SG, Lee R. Optimization of energy modulation filter for dual energy CBCT using Geant4 Monte-Carlo simulation. Prog Med Phys. 2016;27:125-130.
6. Hutton BF. Recent advances in iterative reconstruction for clinical SPECT/PET and CT. Acta Oncol. 2011;50:851-858.
7. Geyer LL, Schoepf UJ, Meinel FG, Nance JW Jr, Bastarrika G, Leipsic JA, et al. State of the Art: iterative CT reconstruction techniques. Radiology. 2015;276:339-357.
8. Greffier J, Larbi A, Frandon J, Daviau PA, Beregi JP, Pereira F. Influence of iterative reconstruction and dose levels on metallic artifact reduction: a phantom study within four CT systems. Diagn Interv Imaging. 2019;100:269-277.
9. Kuo Y, Lin YY, Lee RC, Lin CJ, Chiou YY, Guo WY. Comparison of image quality from filtered back projection, statistical iterative reconstruction, and model-based iterative reconstruction algorithms in abdominal computed tomography. Medicine (Baltimore). 2016;95:e4456.
10. Bernard A, Comby PO, Lemogne B, Haioun K, Ricolfi F, Chevallier O, et al. Deep learning reconstruction versus iterative reconstruction for cardiac CT angiography in a stroke imaging protocol: reduced radiation dose and improved image quality. Quant Imaging Med Surg. 2021;11:

392-401.

11. Lenfant M, Chevallier O, Comby PO, Secco G, Haioun K, Ricolfi F, et al. Deep learning versus iterative reconstruction for CT pulmonary angiography in the emergency setting: improved image quality and reduced radiation dose. Diagnostics (Basel). 2020;10:558.
12. Kawashima H, Ichikawa K, Matsubara K, Nagata H, Takata T, Kobayashi S. Quality evaluation of image-based iterative reconstruction for CT: comparison with hybrid iterative reconstruction. J Appl Clin Med Phys. 2019;20:199-205.
13. Peng C, Qiu B, Li M, Guan Y, Zhang C, Wu Z, et al. Gaussian diffusion sinogram inpainting for X-ray CT metal artifact reduction. Biomed Eng Online. 2017;16:1.
14. Chun M, Choi YH, Kim JH. Automated measurement of CT noise in patient images with a novel structure coherence feature. Phys Med Biol. 2015;60:9107-9122.
15. Nakaura T, Awai K, Oda S, Funama Y, Harada K, Uemura S, et al. Low-kilovoltage, high-tube-current MDCT of liver in thin adults: pilot study evaluating radiation dose, image quality, and display settings. AJR Am J Roentgenol. 2011; 196:1332-1338.
16. Lin PJP, Beck TJ, Borras C, Cohen G, Jucius RA, Kriz RJ, et al. AAPM report No. 39. Specification and acceptance testing of computed tomography scanners. Alexandria: American Association of Physicists in Medicine; 1993.
17. Tian X, Samei E. Accurate assessment and prediction of noise in clinical CT images. Med Phys. 2016;43:475.
18. Christianson O, Winslow J, Frush DP, Samei E. Automated technique to measure noise in clinical CT examinations. AJR Am J Roentgenol. 2015;205:W93-W99.
19. Onoue K, Yakami M, Nishio M, Sakamoto R, Aoyama G, Nakagomi K, et al. Temporal subtraction CT with nonrigid image registration improves detection of bone metastases by radiologists: results of a large-scale observer study. Sci Rep. 2021;11:18422.
20. Li M, Zheng J, Zhang T, Guan Y, Xu P, Sun M. A prior-based metal artifact reduction algorithm for x-ray CT. J Xray Sci Technol. 2015;23:229-241.
21. Subhas N, Primak AN, Obuchowski NA, Gupta A, Polster JM, Krauss A, et al. Iterative metal artifact reduction: evaluation and optimization of technique. Skeletal Radiol. 2014; 43:1729-1735.
22. Große Hokamp N, Eck B, Siedek F, Pinto Dos Santos D, Holz JA, Maintz D, et al. Quantification of metal artifacts in computed tomography: methodological considerations. Quant Imaging Med Surg. 2020;10:1033-1044.
23. Prell D, Kyriakou Y, Struffert T, Dörfler A, Kalender WA. Metal artifact reduction for clipping and coiling in interventional C-arm CT. AJNR Am J Neuroradiol. 2010;31:634-639.
24. Fukui R, Matsuura R, Kida K, Goto S. Effect of the number of projected images on the noise characteristics in tomosynthesis imaging. Prog Med Phys. 2021;32:50-58.
25. Prakash P, Kalra MK, Kambadakone AK, Pien H, Hsieh J, Blake MA, et al. Reducing abdominal CT radiation dose with adaptive statistical iterative reconstruction technique. Invest Radiol. 2010;45:202-210.
26. Mileto A, Guimaraes LS, McCollough CH, Fletcher JG, Yu L. State of the Art in abdominal CT: the limits of iterative reconstruction algorithms. Radiology. 2019;293:491-503.
27. McCollough CH, Yu L, Kofler JM, Leng S, Zhang Y, Li Z, et al. Degradation of CT low-contrast spatial resolution due to the use of iterative reconstruction and reduced dose levels. Radiology. 2015;276:499-506.
28. Goenka AH, Herts BR, Obuchowski NA, Primak AN, Dong F, Karim W, et al. Effect of reduced radiation exposure and iterative reconstruction on detection of low-contrast low-attenuation lesions in an anthropomorphic liver phantom: an 18-reader study. Radiology. 2014;272:154-163.
29. Stephenson I, Saunders A. Simulating film grain using the noise-power spectrum. EG UK Theory and practice of computer graphics. The Eurographics Association; 2007:69-72.